

# Long-term aerobic cometabolism of a chlorinated solvent mixture by vinyl chloride-, methane- and propane-utilizing biomasses

Dario Frascari<sup>a,\*</sup>, Davide Pinelli<sup>a</sup>, Massimo Nocentini<sup>a</sup>, Arianna Zannoni<sup>a</sup>, Stefano Fedi<sup>b</sup>, Emilia Baleani<sup>b</sup>, Davide Zannoni<sup>b</sup>, Angiolo Farneti<sup>c</sup>, Alfredo Battistelli<sup>c</sup>

<sup>a</sup> Department of Chemical, Mining and Environmental Engineering, University of Bologna, Via Terracini 34, Bologna 40131, Italy

<sup>b</sup> Department of Experimental and Evolutionistic Microbiology, University of Bologna, Via Selmi 3, Bologna, Italy

<sup>c</sup> Snamprogetti SpA, Divisione Aquater (ENI Group), Via Toniolo 1, Fano, PU 61032, Italy

Received 24 November 2005; received in revised form 28 April 2006; accepted 2 May 2006

Available online 9 May 2006

## Abstract

The aerobic cometabolic biodegradation of a mixture of chlorinated aliphatic hydrocarbons (CAHs) including vinyl chloride (VC), *cis*- and *trans*-1,2-dichloroethylene (*cis*-DCE, *trans*-DCE), trichloroethylene (TCE), 1,1,2-trichloroethane (1,1,2-TCA) and 1,1,2,2-tetrachloroethane (1,1,2,2-TeCA) was investigated at both 25 and 17 °C by means of bioaugmented and non-bioaugmented sediment-groundwater slurry microcosm tests. The goals of the study were (i) to study the long-term aerobic biodegradation of a CAH mixture including a high-chlorinated solvent (1,1,2,2-TeCA) generally considered non-biodegradable in aerobic conditions; (ii) to investigate the efficacy of bioaugmentation with two types of internal inocula obtained from the indigenous biomass of the studied site; (iii) to identify the CAH-degrading bacteria. VC, methane and propane were utilized as growth substrates. The non-bioaugmented microcosms were characterized, at 25 °C, by an average 18-day lag-time for the direct metabolism of VC (accompanied by the cometabolism of *cis*- and *trans*-DCE) and by long lag-times (36–264 days) for the onset of methane or propane utilization (associated with the cometabolism of the remaining CAHs). In the inoculated microcosms the lag-phases for the onset of growth substrate utilization and CAH cometabolism were significantly shorter (0–15 days at 25 °C). Biodegradation of the 6-CAH mixture was successfully continued for up to 410 days. The low-chlorinated solvents were characterized by higher depletion rates. The composition of the microbial consortium of a propane-utilizing microcosm was determined by 16s rDNA sequencing and phylotype analysis. To the best of our knowledge, this is the first study that documents the long-term aerobic biodegradation of 1,1,2,2-TeCA.

© 2006 Elsevier B.V. All rights reserved.

**Keywords:** Chlorinated solvent; Chlorinated aliphatic hydrocarbon; Biodegradation; Cometabolism; Bioaugmentation

## 1. Introduction

Chlorinated aliphatic hydrocarbons (CAHs) are widespread subsurface contaminants that are often present in polluted sites as complex mixtures [1,2]. Several studies showed that most CAHs can be biodegraded via aerobic cometabolism by single bacterial strains or mixed microbial populations grown on aromatic and aliphatic hydrocarbons such as methane, propane, butane, phenol or toluene. While most studies monitored the aerobic biodegradation of single CAHs (e.g. [3–7]) or the short-term transformation of binary or ternary CAH mixtures [1,2,8,9], the long-term aerobic biodegradation of complex CAH mix-

tures was investigated in a limited number of studies (e.g. [10,11]). High-chlorinated CAHs, such as carbon tetrachloride (CT), 1,1,1,2- and 1,1,2,2-tetrachloroethane (1,1,1,2- and 1,1,2,2-TeCA) and perchloroethylene (PCE) are generally considered non-biodegradable in aerobic conditions [12–14]. Several studies also evidenced that some low-chlorinated CAHs can be transformed via aerobic direct metabolism, and that some aerobic strains grown on vinyl chloride (VC) can degrade *cis*- and *trans*-1,2-dichloroethylene (*cis*- and *trans*-DCE) via cometabolism [15–18].

Bioaugmentation is a powerful tool for enhancing the aerobic cometabolic CAH biodegradation [19–21]. In particular, it can be aimed at inducing the rapid onset of the degradation activity in those cases where the site's indigenous biomass would require a long lag-phase before starting the cometabolic transformation process. Because in situ bioaugmentation with exogenous

\* Corresponding author. Tel.: +39 0512090416; fax: +39 0516347788.  
E-mail address: dario.frascari@unibo.it (D. Frascari).

Table 1  
Temperature and added compounds in the seven groups of microcosms

Group of microcosms	Set up day	Microcosm label	Temperature (°C)	Added primary substrate		Added nutrients	
				Type	Aq. phase concentration (μM)	Nitrate (μmol N)	Phosphate (μmol P)
VC (indigenous biomass + VC)	0	VC 1, 2	25	VC	25	32	1.1
		VC 3, 4	25		25	–	–
		VC 5, 6	17		31	32	1.1
M (indigenous biomass + methane + VC)	0	M 1, 2 <sup>a</sup>	25	CH <sub>4</sub> , VC	125, 25	128	4.3
		M 7, 8	25		31, 25	32	1.1
		M 3, 4	25		125, 25	–	–
		M 5, 6	17		144, 31	128	4.3
P (indigenous biomass + propane + VC)	0	P 1, 2	25	C <sub>3</sub> H <sub>8</sub> , VC	46, 25	128	4.3
		P 7, 8	25		11, 25	32	1.1
		P 3, 4	25		46, 25	–	–
		P 5, 6	17		50, 31	128	4.3
I-M (indigenous inoculum from microcosm M4 + methane + VC)	152	I-M 1, 2	25	CH <sub>4</sub> , VC	125, 25	–	–
		I-M 3, 4	17		144, 31	–	–
I-P (indigenous inoculum from microcosm P2 + propane + VC)	223	I-P 1, 2	25	C <sub>3</sub> H <sub>8</sub> , VC	46, 25	–	–
		I-P 3, 4	17		50, 31	–	–
C <sup>b</sup>	0	C1	25	VC	25	–	–
		C2	25	CH <sub>4</sub> , C <sub>3</sub> H <sub>8</sub> , VC	125, 46, 25	–	–

<sup>a</sup> At day 224 microcosm M2 was inoculated with biomass taken from M4. Therefore, relatively to the data obtained after that time, it is considered as belonging to group I-M.

<sup>b</sup> Sterile controls for abiotic reactions and losses due to absorption in the septa or sampling procedures. Sterilized with NaN<sub>3</sub> 57 mM.

inocula is in some countries not easily accepted by the control authorities, the utilization of indigenous inocula represents an interesting field of investigation.

In this microcosm study we investigated the long-term aerobic cometabolic degradation of a mixture of six CAHs including a high-chlorinated compound (1,1,2,2-TeCA) by mixed microbial cultures grown on VC, methane or propane. The microcosms were set up with soil and groundwater sampled from an industrial CAH-contaminated site. We examined the efficacy of bioaugmentation with two types of indigenous inocula, and we evaluated the long-term CAH depletion rates in slurry conditions. Finally, the 16s rDNA of the microbial consortium of one of the best-performing reactors was analyzed following total DNA extraction and PCR amplification.

## 2. Materials and methods

### 2.1. Experimental scheme and microcosm set up

The study was conducted in aerobic slurry batch microcosms, prepared using 119-mL bottles with Teflon-lined rubber septa. Each microcosm contained 20 g of soil (sand 48%, silt 46%, clay 6%) and 50 mL of brackish groundwater taken from a site contaminated by VC, *cis*-DCE, *trans*-DCE, trichloroethylene (TCE), 1,1,2-trichloroethane (1,1,2-TCA) and 1,1,2,2-TeCA. The 59-mL headspace was filled with air. To avoid bacterial contamination, bottles, caps and all the tools used for microcosm preparation were autoclaved (121 °C, 20 min).

The experimental scheme, consisting of 15 operational conditions studied in duplicate microcosms plus 2 control conditions (sterilized with NaN<sub>3</sub>) and reported in Table 1, was designed to take into account four variables: temperature (17 or 25 °C<sup>1</sup>), concentration of macro-nutrients (N and P), effect of the addition of microbial inocula and type and concentration of primary substrate. In particular, in microcosm group VC, vinyl chloride was the only substrate supplied, whereas in groups M and P, in addition to VC, methane (group M) and propane (group P) were supplied, in order to investigate the effectiveness of these growth substrates in stimulating the biodegradation of a CAH mixture that includes VC. When active bacterial consortia began to develop in the M and P microcosms, inocula were taken from reactors M4 ( $1 \times 10^6$  CFU mL<sup>-1</sup>) and P2 ( $4 \times 10^5$  CFU mL<sup>-1</sup>) and utilized to set up two further sets of microcosms, I-M and I-P, in order to investigate the effect of the inoculation on the lag-times for the onset of the CAH mixture biodegradation process and on the depletion rates achievable in slurry conditions. The inocula were performed by introducing 1 mL of suspension sampled from the parent microcosm with a sterile syringe in a newly set up microcosm. The initial aqueous-phase concentrations of the CAHs and of other significant groundwater constituents at 25 and 17 °C are reported in Table 2.

<sup>1</sup> A 17 °C is the average yearly temperature of the aquifer where the soil and groundwater were sampled. Several tests were performed at 25 °C in order to speed up the biodegradation processes and to obtain an indication of the effect of temperature on the CAH degradation rates.

## 2.2. Analysis and chemicals

The CAHs and propane were purchased from Aldrich (Gillingham, UK), whereas methane was taken from the distribution network of the local gas company. Purities were: propane, VC and TCE, 99.5%; 1,1,2-TCA, 99%; *trans*-DCE, 1,1,2,2-TeCA and methane, 98%; *cis*-DCE, 97%. The gas-phase concentrations of methane, propane and CAHs were measured with a HP6890 gas chromatograph equipped with a capillary HP-VOC column (30 m × 0.32 mm) connected to a flame ionization detector (250 °C) for the analysis of methane, propane and VC and to an electron capture detector (250 °C) for the analysis of the remaining CAHs (injector temperature 250 °C; injection volume 500- $\mu$ L; split ratio 10:1; oven temperature 3 min at 60 °C, ramp to 230 °C at 20 °C/min, 5 min at 230 °C; carrier gas He at 0.9 mL/min). To avoid microbial cross contamination, before each analysis the syringe was kept in the GC injector (250 °C) for about 1 min and subsequently filled twice with hot gas from the GC injector. Detection limits were ( $\mu$ M in the aq. phase): methane and propane, 0.007; VC, 1.2; *trans*-DCE, 0.08; *cis*-DCE, 0.15; TCE,  $4 \times 10^{-6}$ ; 1,1,2-TCA, 0.01; 1,1,2,2-TeCA, 0.02. The standard methods [22] were applied for the analysis of pH, Cl<sup>-</sup>, SO<sub>4</sub><sup>2-</sup>, NH<sub>3</sub>-N, NO<sub>3</sub><sup>-</sup>-N, P, Fe and Mn. All the methods were calibrated with external standards. Total masses and aqueous phase concentrations were calculated utilizing the gas/liquid and solid/liquid equilibrium constants estimated at 25 or 17 °C [23,24]. Bacterial plate counts were performed as described by Frascari et al. [25]. Total DNA extraction and

purification, 16S rDNA amplification, cloning and sequencing of microbial consortia were performed as described by Fedi et al. [26].

## 2.3. Microcosm operation

In microcosm groups M, P, I-M and I-P, after the onset of methane or propane utilization, these substrates were supplied in consecutive spikes (5.4 mL of methane or 1.85 mL of propane, at a room temperature of 20–22 °C) corresponding to average feed rates of about 4 mg<sub>C</sub>/week. The initial methane or propane concentration in each consecutive pulse was that reported in Table 1 except for microcosms M7, M8, P7, P8, where the subsequent pulses were characterized by initial concentrations equal to those reported in Table 1, respectively, for microcosms M1, M2, P1 and P2. Ammonium (as NH<sub>4</sub>Cl) and phosphate (as KH<sub>2</sub>PO<sub>4</sub> and K<sub>2</sub>HPO<sub>4</sub> at 0.65:1 weight ratio) were periodically added, so as to prevent N and P from being limiting factors for bacterial growth. Each time all the six CAHs were completely degraded, they were re-introduced by spiking 60–120  $\mu$ L of gaseous VC and 15–40  $\mu$ L of a concentrated aqueous solution of *cis*-DCE (9720  $\mu$ M), *trans*-DCE (10 940  $\mu$ M), TCE (5260  $\mu$ M), 1,1,2-TCA (1540  $\mu$ M) and 1,1,2,2-TeCA (900  $\mu$ M). The CAH amount introduced in a given microcosm was varied from pulse to pulse in order to study – limitedly to low-concentration ranges – the effect of concentration on the transformation rates. Table 2 shows the ranges of variation of the CAH initial concentrations in the pulses. As a consequence of these operational procedures, in the four microcosm groups amended with methane or propane the VC average feed rate was about 150 times lower than the average methane or propane feed rate. Therefore, the biomasses developed in these microcosms can be considered primarily as methane- or propane-growing, although they might include small fractions of VC-growing strains. During each pulse of the 6-CAH mixture, the amount of each compound lost as a result of the headspace samplings for GC analysis (as an average, 10 500- $\mu$ L samplings in each pulse) varied between 0.15% (for 1,1,2,2-TeCA) and 4.7% (for VC) of the total amount depleted. Therefore, the lower frequency of headspace samplings in the sterilized controls with respect to the viable microcosms did not significantly affect the comparison of the CAH depletion rates calculated for the two types of microcosms. Aqueous phase samplings were always performed in the absence of CAHs. Prior to each primary substrate supply oxygen (7.5–9 mL) was supplied with a frictionless glass syringe, so as to maintain aerobic conditions and to compensate the pressure decrease due to the headspace samplings for GC analysis and to the reaction of oxidation of the primary substrate to CO<sub>2</sub>. The utilization of a frictionless syringe allowed to introduce oxygen until the attainment of atmospheric pressure in the microcosms. Following oxygen addition, the supply of methane or propane led to a small overpressure in the microcosm headspace. As a result of this operational procedure, the headspace pressure in the microcosms followed within each pulse of primary substrate consumption a cyclic trend with variations between 1.10 and 0.90 atm (1.03–0.90 atm in the propane-fed tests). During the phases of headspace pressure higher than 1 atm, the CAH analytical proce-

Table 2  
Chlorinated solvents and other significant groundwater constituents: initial concentrations in the microcosm aqueous phase

Parameter	Initial concentration <sup>a</sup> ( $\mu$ M)	
	Tests at 25 °C	Tests at 17 °C <sup>b</sup>
VC	25 (20–41) <sup>c</sup>	31 (25–51) <sup>c</sup>
<i>Trans</i> -DCE	3.4 (2.2–5.8) <sup>c</sup>	3.9 (2.5–6.5) <sup>c</sup>
<i>Cis</i> -DCE	3.1 (2.3–6.2) <sup>c</sup>	3.3 (2.5–6.7) <sup>c</sup>
TCE	1.9 (1.0–2.7) <sup>c</sup>	2.2 (1.2–3.1) <sup>c</sup>
1,1,2-TCA	0.30 (0.41–1.08) <sup>c</sup>	0.31 (0.41–1.09) <sup>c</sup>
1,1,2,2-TeCA	0.15 (0.24–0.65) <sup>c</sup>	0.15 (0.24–0.65) <sup>c</sup>
pH <sup>d</sup>	6.5	6.5
Cl <sup>-</sup>	366000	366000
SO <sub>4</sub> <sup>2-</sup>	7800	7800
NH <sub>3</sub> -N	14500	14500
NO <sub>3</sub> <sup>-</sup> -N	<550	<550
P	<3	<3
Fe	1.8	1.8
Mn	4.0	4.0

<sup>a</sup> The initial concentration of each CAH in the microcosm aqueous phase results from the equilibrium partitioning into the three phases of the amount of CAH initially present in the soil and groundwater plus the following initial additions: 40  $\mu$ L of VC; 10  $\mu$ L of a stock solution of *trans*-DCE (7380  $\mu$ M) and TCE (4410  $\mu$ M) in water.

<sup>b</sup> In the tests at 17 °C, as a consequence of the addition, in each pulse, of the same mass of each CAH as in the tests at 25 °C, CAH concentrations were higher than in the 25 °C tests.

<sup>c</sup> The interval of variation of the initial concentration in the subsequent pulses is reported in parenthesis.

<sup>d</sup> pH units.

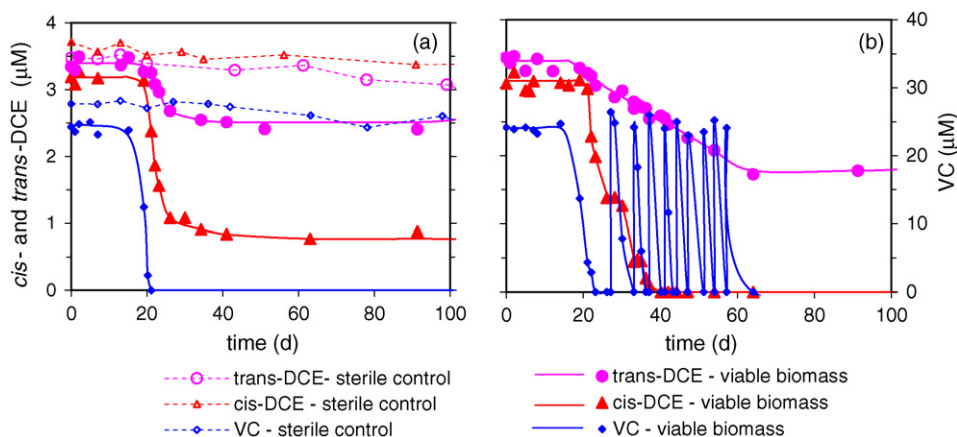


Fig. 1. VC uptake and cometabolic biodegradation of *cis*- and *trans*-DCE by VC-utilizing biomasses in a microcosm with a single VC spike (a) and in one with subsequent VC re-spikes (b): aqueous phase concentrations vs. time, and interpolating lines. In part (a), the VC, *cis*-DCE and *trans*-DCE concentrations measured in the sterile controls during the first 100 days of operation are also shown.

dures resulted, at the most, in a 9% underestimation of the actual headspace concentration (3% in the propane-fed tests). In order to remove CO<sub>2</sub> and possible volatile toxic degradation products, the aqueous phases of all microcosms were periodically stripped (in the absence of CAHs) for 15 min with 0.2 µm-filtered air introduced with a sterile needle. Microcosms were kept in continuous agitation in two rollers operated at 3.3 rpm and maintained, respectively, at 25 ± 0.5 and 17 ± 0.5 °C, and were operated for a time variable between 90 and 450 days.

#### 2.4. Estimation of lag-times and degradation rates

The lag-times for the onset of primary substrate consumption and CAH degradation were obtained by the intersection of the maximum slope line of the concentration–time curve with the horizontal line passing through the initial concentration value. Each pulse was characterized by the maximum degradation rate relative to each substance, calculated by dividing the maximum slope of the mass–time curve by the volume of the liquid phase. Each degradation rate was associated with the aqueous phase concentration corresponding to the initial value of the portion of the mass–time curve utilized to calculate the degradation rate. The uncertainties relative to average lag-times, degradation rates and total amounts degraded are reported as 95% confidence intervals.

### 3. Results and discussion

#### 3.1. CAH depletion in the sterilized controls

The CAH initial depletion rates obtained at 25 °C in the sterilized control microcosms, reported in detail in SI-1 in the Electronic Supplementary Material together with the corresponding initial concentrations, varied between 0.7 nmol L<sub>aq. phase</sub><sup>-1</sup> d<sup>-1</sup> (for 1,1,2-TCA) and 95 nmol L<sub>aq. phase</sub><sup>-1</sup> d<sup>-1</sup> (for VC). The comparison between these rates and the depletion rates obtained in the viable microcosms is reported and commented in Sections 3.2–3.4. The CAH concentration profiles in the sterilized controls fol-

lowed a first-order kinetic. The best estimates of the first-order constants, reported in SI-1, correspond to abiotic half-lives varying between 2 months (for TCE and 1,1,2,2-TeCA) and 2.5 years (for *cis*-DCE).

#### 3.2. Utilization of VC as primary substrate

As shown in Fig. 1 for two representative microcosms, in all the non-inoculated microcosms (groups VC, M and P) the degradation of VC began after a lag-time variable between 14 and 50 days and before the onset of the microbial uptake of methane or propane (where present), and rapidly proceeded until complete VC depletion. The VC lag-time resulted independent of the presence and concentration of methane, propane or added nutrients but strongly influenced by temperature, with an average value of 18 ± 1 days at 25 °C and of 43 ± 3 days at 17 °C. These results are in agreement with numerous studies on direct VC metabolism [15,17,18] indicating that aerobic VC-utilizing bacteria are relatively common in soils and that the onset of the process is typically characterized by a lag-phase of some weeks. As shown in Fig. 1b for a representative case, in 10 of the 22 non-inoculated microcosms the VC degradation process was maintained for about 45 days (25 days in the tests at 17 °C) by introducing consecutive spikes (2.9 µmol<sub>VC</sub>) corresponding to a mass rate of about 0.13 mg<sub>C</sub>/week. Fig. 2 shows that the VC rate increased with increasing VC mass degraded, suggesting that VC was utilized as the growth substrate. As an average, the VC rate at 17 °C was 60% lower than that at 25 °C. The VC aqueous phase concentrations measured in a sterile control during the initial 100 days of operation are compared in Fig. 1a with the corresponding concentrations obtained in a viable microcosm characterized by the supply of a single VC pulse. The VC depletion rate obtained in the sterilized control microcosms (at 25 °C and at an average 29.5 µM initial concentration) corresponds to 0.5% of the highest VC rate obtained, at the same temperature and at a slightly lower initial concentration, in the VC-utilizing microcosms, indicating that abiotic reactions (such as hydrolysis) and losses through caps gave a negligible contribution to the VC rates attained in the viable microcosms. In the inocu-

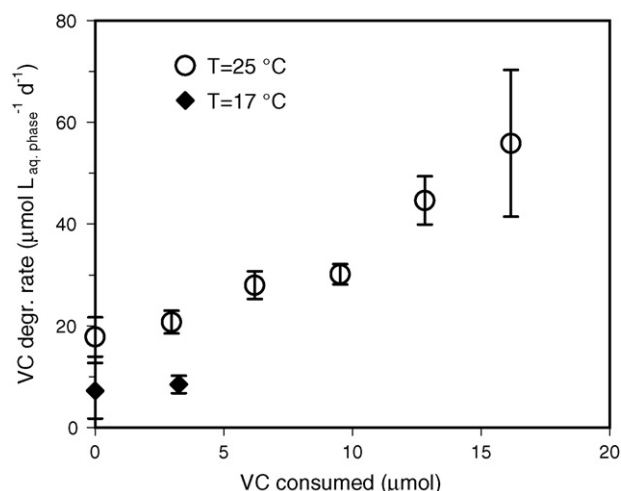


Fig. 2. Average VC degradation rate vs. cumulative VC mass degraded, with 95% confidence intervals.

lated microcosms (groups I-M and I-P), as reported in detail in Table 4, the onset of VC degradation was characterized by a short lag-time and by the contemporary onset of methane or propane utilization. A representative example of VC concentration versus time in an inoculated methane-utilizing microcosm is shown in the upper part of SI-2 in the Electronic Supplementary Material.

### 3.3. Cometabolic degradation of *cis*-DCE and *trans*-DCE by VC-growing cultures

As shown for two representative microcosms in Fig. 1, in all the microcosms where direct metabolism of VC took place, the contemporary depletion of *cis*-DCE and *trans*-DCE was

observed. At 25 °C, the *cis*-DCE degradation rate varied between 0.24 and 1.0 µmol L<sub>aq. phase</sub><sup>-1</sup> d<sup>-1</sup>, with an average molar ratio of *cis*-DCE rate to VC rate of 3.2% ± 0.9% (in correspondence with an average ratio of *cis*-DCE to VC initial concentration equal to 0.14). The *cis*-DCE and *trans*-DCE aqueous phase concentrations measured in a sterile control during the initial 100 days of operation are compared in Fig. 1a with the corresponding concentrations obtained in a viable microcosm characterized by the supply of a single VC pulse. The *cis*-DCE depletion rate of the sterile controls corresponds to 0.2–1.0% of the *cis*-DCE rates obtained, at the same temperature and initial concentration, in the VC-utilizing microcosms, indicating again the negligible contribution of non-biological processes. In the microcosms where VC was not re-spiked after exhaustion of the amount initially present, 0.10–0.22 µmol of *cis*-DCE were degraded, with a residual 0.72–2.6 µM concentration (Fig. 1a), whereas in the tests where VC was re-spiked, *cis*-DCE degradation proceeded, and was completed in correspondence with the 3rd or 4th VC pulse (Fig. 1b), suggesting that *cis*-DCE was degraded via cometabolism by VC-growing biomasses. In the tests characterized by a residual *cis*-DCE concentration, the ratio of *cis*-DCE moles degraded to VC moles utilized (transformation yield) resulted equal to 4.9% ± 0.3% at 25 °C and 2.8% ± 0.6% at 17 °C. A marked VC inhibition on *cis*-DCE degradation was observed in all microcosms: *cis*-DCE depletion stopped each time VC was re-spiked, and resumed when VC fell below 3–4 µM (Fig. 1b). VC inhibition on *cis*-DCE aerobic cometabolism is reported also by Verce et al. [15].

VC utilization was also accompanied by *trans*-DCE depletion (Fig. 1a and b), with an average rate equal to 0.06 µmol L<sub>aq. phase</sub><sup>-1</sup> d<sup>-1</sup> at 25 °C (7 times higher than the average rate obtained in the sterilized controls). When VC re-spiking was halted the *trans*-DCE rate became equal to the abiotic rate,

Table 3

Lag-times for the onset of primary substrate (methane or propane) uptake and CAH mixture cometabolic biodegradation (days)

Groups of microcosms	Temperature (°C)	Methane-fed microcosms			Propane-fed microcosms		
		Test	Substrate lag-time	CAH mixture lag-time <sup>a</sup>	Test	Substrate lag-time	CAH mixture lag-time <sup>a</sup>
Indigenous biomass (P, M)	25	M1	247	0	P1	139	0
		Test M2 is included in group I-M <sup>b</sup>			P2	102	7
		M3	242	22	P3	77	0
		M4	34	2	P4	132	17
	17	M7	103	0	P7	243	0
		M8	103	0	P8	109	0
		M5	179	39	P5	308	15
		M6	>450 <sup>c</sup>		P6	362	0
Inoculated microcosms (I-P, I-M)	25	I-M1	<1	0	I-P1	10	0
		I-M2	<1	10	I-P2	10	5
		M2 <sup>b</sup>	<1	8			
	17	I-M3	<1	8	I-P3	43	8
I-M4		<1	8	I-P4	43	8	

<sup>a</sup> The CAH-mixture lag-time is defined as the longest of the lag-times relative to the six CAHs and is calculated from the end of the primary substrate (methane or propane) lag-time.

<sup>b</sup> At day 224, M2 was inoculated with biomass taken from M4 in order to test whether the long methane lag-phases could be ascribed to the presence of conditions not favorable for the development of methane-utilizing biomasses.

<sup>c</sup> M6 was still in lag-time when the study was terminated.

Table 4  
Average lag-time of the single CAHs in each group of microcosms

Temperature (°C)	Microcosm group	Average lag-time <sup>a</sup> (day)					
		VC	<i>t</i> -DCE	<i>c</i> -DCE	TCE	1,1,2-TCA	1,1,2,2-TeCA
25	M	b	0	0	0.7	11	0
	P	b	5	0	0	0	0
17	M	b	0	0	39	34	0
	P	b	0	0	4	7	0
25	I-M	0	0.5	0.8	2	5	6
	I-P	0	2	5	0	0	0
17	I-M	0	5	7	3	2	0
	I-P	0	8	0	0	0	0

<sup>a</sup> The lag-time of each CAH is calculated from the end of the primary substrate (methane or propane) lag-time.

<sup>b</sup> VC was not present in any of the non-inoculated microcosms at the onset of substrate uptake, as it had previously been depleted via direct metabolism. When it was re-spiked in subsequent CAH-mixture pulses, its degradation began immediately.

suggesting that also the observed *trans*-DCE disappearance was a cometabolic process. The average ratio of *trans*-DCE mass degraded to VC mass utilized resulted equal to  $2.4\% \pm 0.6\%$  at  $25^\circ\text{C}$  and  $1.4\% \pm 0.3\%$  at  $17^\circ\text{C}$ . No cometabolic degradation of TCE, 1,1,2-TCA or 1,1,2,2-TeCA by VC-growing biomasses occurred.

#### 3.4. Lag-times for the onset of the cometabolic biodegradation of the CAH mixture by propane- and methane-utilizing biomasses

In 23 of the 24 microcosms amended with either methane or propane (groups M, P, I-M and I-P) the onset of consumption of the main substrate supplied was observed within at the latest 1 year, and was followed by the onset of the degradation of the CAH mixture. Conversely, in one of the methane-fed non-inoculated microcosms (M6), no significant substrate consumption had been observed at the end of the study (day 450). Table 3 reports the growth substrate (methane or propane) lag-time and the CAH-mixture lag-time (calculated from the end of the growth substrate lag-time and defined as the longest of the lag-times relative to the 6 CAHs) observed in each microcosm.

The detailed lag-times of each CAH are reported in Table 4 in terms of average value in each group of microcosms. The initial pulse of the CAH mixture in a non-inoculated M-type microcosm is shown in Fig. 3, whereas the initial three pulses of the CAH mixture in an inoculated I-M type microcosm are shown in SI-2 in the Electronic Supplementary Material. It can be observed in Fig. 3 that while VC consumption, accompanied by a decrease in *cis*- and *trans*-DCE concentration, occurred before the onset of methane utilization (day 20), at day 34 the start of methane uptake was rapidly followed by the onset of TCE, 1,1,2-TCA and 1,1,2,2-TeCA biodegradation and by the completion of *cis*- and *trans*-DCE depletion.

In the non-inoculated tests (P and M), the onset of substrate uptake proved to be the limiting step, with lag-phases ranging between 36 and more than 450 days with a tendency to higher values at  $17^\circ\text{C}$  and without any significant effect of substrate or macro-nutrients initial concentration. The CAH-mixture lag-time was zero in most tests, and significantly shorter than the substrate lag-phase in the remaining cases. Where present, the CAH lag-time was due to *trans*-DCE, TCE or 1,1,2-TCA, with a tendency to longer lag-times at  $17^\circ\text{C}$  (Table 4). The bioaugmented microcosms resulted in significantly shorter lag-times

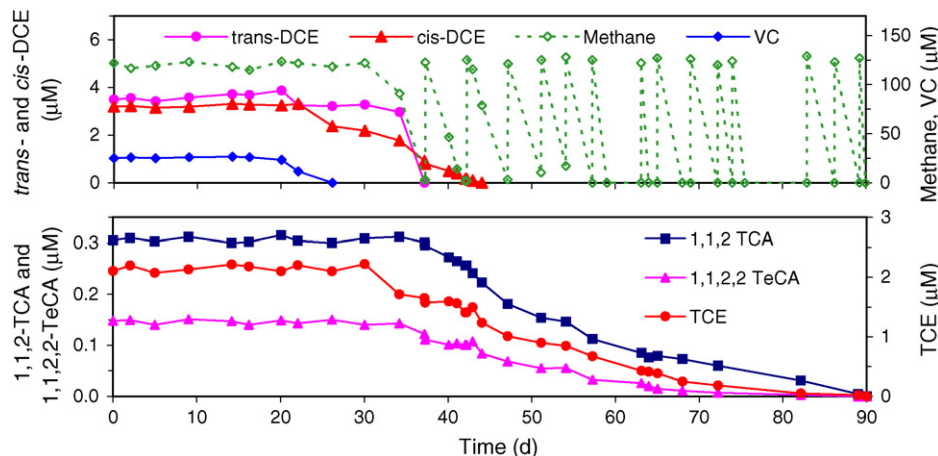


Fig. 3. CAH and methane aqueous phase concentrations vs. time during the initial pulse of the CAH mixture in a microcosm (M4) characterized by a 20-day VC lag-time, a 34-day methane lag-time and by a 2-day CAH mixture lag-time.

Table 5

Average methane or propane utilization rate and average culturable biomass concentration in each microcosm group  $\pm$  95% confidence intervals

	Temperature ( $^{\circ}$ C)	Microcosm group	Primary substrate (methane or propane) utilization rate ( $\text{mg}_C \text{L}_{\text{aq. phase}}^{-1} \text{d}^{-1}$ )	Culturable biomass concentration <sup>a</sup>
Indigenous biomass	25	M	$55 \pm 3$	$6.2 \times 10^6 \pm 2.5 \times 10^6$
		P	$56 \pm 5$	$5.3 \times 10^6 \pm 1.8 \times 10^6$
	17	M	$31 \pm 6$	b
		P	$33 \pm 5$	b
Inoculated microcosms	25	I-M	$53 \pm 8$	$1.5 \times 10^6 \pm 6.5 \times 10^5$
		I-P	$57 \pm 5$	$1.1 \times 10^6 \pm 4.4 \times 10^5$
	17	I-M	$33 \pm 7$	b
		I-P	$38 \pm 0.7$	b

<sup>a</sup> Total aerobic heterotrophs ( $\text{CFU mL}^{-1}$ ).<sup>b</sup> Not enough biomass measurements available.

than the non-inoculated ones (0–15 days at  $25^{\circ}\text{C}$ ), with the best performance in the I-M group (0–10 days at  $25^{\circ}\text{C}$ ) and with CAH lag-times due, in the propane-fed tests, only to *trans*-DCE, and in the methane-fed to all the CAHs present. The substrate lag-times we obtained in the non-inoculated assays are significantly longer than those reported for the same substrates in similar studies, which are in the 5–25 days range [27,28].

### 3.5. Cometary biodegradation of the CAH mixture by methane- and propane-utilizing biomasses

After the onset of the biodegradation processes, the entire 6-CAH mixture was completely degraded in all the methane- and propane-utilizing microcosms. After three to six pulses of methane or propane uptake (8–16  $\text{mg}_C$  utilized), all microcosms reached a pseudo steady-state value of substrate utilization rate and culturable biomass concentration, reported in Table 5 in

terms of average value in each microcosm group. Both parameters were quite uniform within each group of microcosms (as indicated by the low 95% confidence intervals). The average substrate rate proved to be significantly affected by temperature (with a 39% average decrease from  $25$  to  $17^{\circ}\text{C}$ ), but not by the type of substrate or by the supply of inoculum. The average biomass concentration was not markedly affected by the type of substrate, but it proved lower (although of the same order of magnitude) in the inoculated microcosms with respect to the non-inoculated ones. A representative trend of total heterotrophic biomass concentration versus time in a microcosm of group M is reported in SI-3 in the Electronic Supplementary Material.

The CAH mixture biodegradation was carried on in the methane-fed reactors for up to 15 CAH pulses (410 days of active CAH degradation) and in the propane-fed reactors for up to 11 pulses (310 days of CAH degradation). The depletion

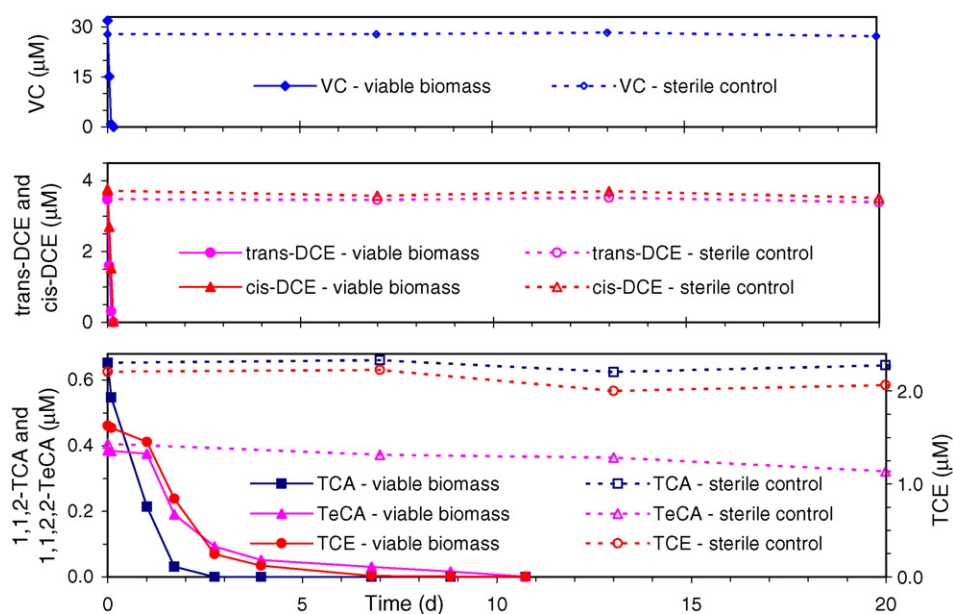


Fig. 4. CAH aqueous phase concentrations during a representative CAH pulse in a methane-fed microcosm, and corresponding concentrations in a sterilized control microcosm during the initial 20 days of operation. For simplicity, daily methane pulses are not shown, and the time relative to the methane-fed microcosm was set to zero at the onset of the CAH pulse.

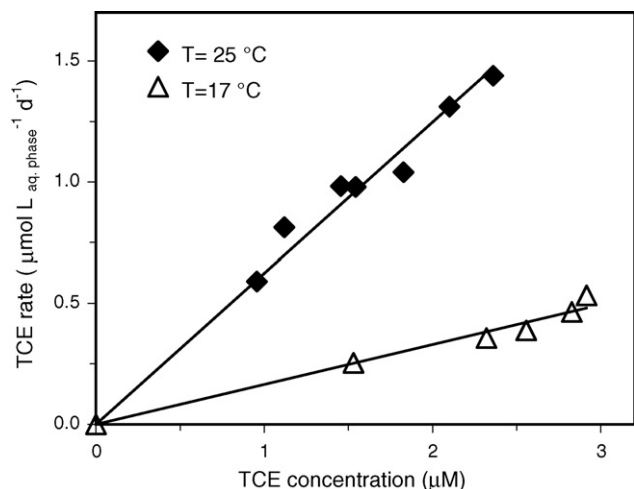


Fig. 5. Rate-concentration plots relative to the depletion of TCE in the I-M microcosms at 17 and 25 °C.

rate of each contaminant was characterized in most microcosms by sharp pulse-to-pulse increases during the initial two to three CAH pulses: for example, in the representative case reported in SI-2 in the Electronic Supplementary Material the ratio of depletion rate in the third CAH pulse to depletion rate in the first CAH pulse varied between 4.4 (for VC) and 99 (for 1,1,2,2-TeCA). Subsequently, in each microcosm the CAH depletion rates attained a stationary condition, characterized, for each CAH, by a maximum depletion rate in each pulse depending on the initial concentration of the compound. This result indicates that in both types of reactors we developed microbial consortia able to perform a sustainable long-term degradation of a 6-CAH mixture. The CAH aqueous phase concentrations during a representative CAH pulse are shown in Fig. 4, together with the corresponding concentrations measured in the sterile controls during the initial 20 days of operation. It can be observed in Fig. 4 that the TCE and 1,1,2-TCA depletion rates are characterized by a sharp increase about 1 day after the onset of the CAH pulse: this behavior is probably due to mutual inhibition among the CAHs, although this aspect was not specifically investigated in this study. The average ratio of total CAH mass degraded to growth substrate mass utilized (transformation yield) was equal to 0.4% (0.06% if expressed as mol/mol) in the methane-fed microcosms and to 0.5% (0.2% if expressed as mol/mol) in the propane-fed microcosms.<sup>2</sup>

In order to compare the long-term depletion rates obtained for the six CAHs in the different experimental conditions tested we constructed a rate-concentration plot for each contaminant/microcosm group/temperature combination, for a total of 60 plots. As an example, the TCE rate-concentration plots relative to the I-M microcosms at 17 and 25 °C are shown in Fig. 5. All the plots were satisfactorily interpolated with linear regressions. This result, given the roughly equal biomass concentrations obtained in the different microcosms of each group (Table 5), indicates that a first-order kinetic model can be

applied to the specific CAH transformation rates in our concentration ranges. The first-order hypothesis is in agreement with the observation that the CAH half-saturation constants reported in the literature are typically higher than the concentration ranges investigated in this study [29–31]. Thus, we utilized the slope of the linear rate-concentration regressions as an index to compare the CAH rates obtained in the different microcosm groups. As observable in Fig. 6, which reports the results obtained at 25 °C, the slopes are characterized, within each microcosm group, by a progressive decrease as the number of chlorine atoms in the solvent increases, with a difference of more than one order of magnitude between VC and 1,1,2,2-TeCA. The only exception to this trend is represented, in the two propane-fed groups, by the *trans*-DCE slopes, which are lower than the slopes of any other solvent in these two microcosm groups. Overall, the methane-utilizing biomasses were more effective towards *trans*-DCE, whereas the propane-utilizing consortia gave better results with TCE, 1,1,2-TCA, 1,1,2,2-TeCA and, secondarily, *cis*-DCE. For both primary substrates, the slopes obtained in microcosm groups I-M and I-P, despite the lower biomass concentrations measured in these microcosms, are equal or higher than those obtained in the parent non-inoculated microcosm groups M and P, respectively, suggesting the attainment of higher specific CAH degradation rates in the inoculated microcosms. The slopes estimated for the 17 °C-microcosms, shown in SI-4 in the Electronic Supplementary Material, follow analogous trends. The reduction of the estimated slope due to the 8 °C temperature decrease varied between 41% (average in group I-P) and 61% (average in group I-M).

Table SI-5 in the Electronic Supplementary Material reports, for each CAH and microcosm group, the ratio between the initial depletion rate in the sterile controls and the corresponding depletion rate in the viable microcosms evaluated, by application of the first-order constants reported in Fig. 6 (25 °C), at the initial concentration of the sterile controls. This ratio is lower than 0.1% in several cases and has a maximum value of 2.7% (for 1,1,2,2-TeCA in microcosm group M), indicating the negligible contribution of abiotic reactions and losses through caps to the depletion rates observed in the microcosms with viable biomass. Given the particularly high concentration of chloride ion in the groundwater utilized (366 mM, or 12 980 mg L<sup>-1</sup>), it was not possible to evaluate the degree of conversion of the organic Cl contained in the CAHs to chloride ion.

While several studies report the anaerobic biodegradation of 1,1,2,2-TeCA, this compound has been generally regarded in the literature as non-biodegradable in aerobic conditions [3,12,14,32,33]. Although its aerobic cometabolic biodegradation by methane-oxidizing cultures was evidenced by a previous work [1], to the best of our knowledge this is the first study that documents the biodegradation of this solvent – even though in a low-concentration range – by propane-oxidizing cultures and that reports its long-term aerobic transformation rates. As indicated in detail in Section 2.3, the headspace samplings and microcosm operational procedure did not affect the TeCA depletion rates obtained in the viable microcosms. The average first-order constants reported in the literature for the two main abiotic reactions of this compound, evaluated at 25 °C and pH

<sup>2</sup> VC was considered a growth substrate in this analysis.



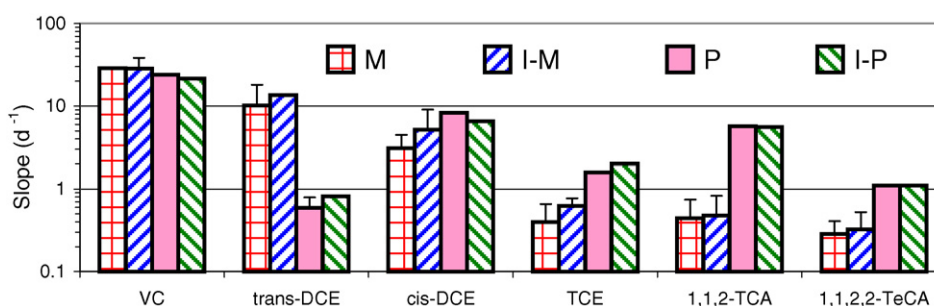


Fig. 6. Slopes of the linear regressions of the rate–concentration plots relative to the microcosms operated at 25 °C. The slopes marked by the 95% confidence interval are those characterized by the presence of at least five rates obtained in the pseudo-stationary condition.

Table 6  
Results of the analysis of the sequenced 16S rDNA of the bacterial consortium of microcosm I-P3

Identification no.	Homology (%)	Reference strain	Reference	Occurrence <sup>a</sup> (%)
AB062106	97	<i>Porphyrobacter sanguineus</i>	[33]	20
AY162047	96	$\alpha$ - <i>Proteobacterium</i> <i>PI.GH2.1.D5</i>	[38]	19
AY690598	99	<i>Roseobacter</i> sp. <i>YSCB-1</i>	<sup>b</sup>	19
AB159609	98	<i>Sphingomonas</i> sp. <i>B9</i>	<sup>b</sup>	11
AF235995	97	$\alpha$ - <i>Proteobacterium</i> <i>F0812</i>	<sup>b</sup>	8
AF407713	98	<i>Uncultured Bacterium</i>	<sup>b</sup>	8
AJ505839	96	$\alpha$ - <i>Proteobacterium</i> <i>A-col-BFA-6</i>	[39]	6
AF245634	93	<i>Uncultured Roseobacter</i> <i>NAC11-6</i>	[36]	3
AF359525	99	<i>Marine Bacterium</i> <i>ATAM407.61</i>	[40]	3
AY258097	100	<i>Bacterium</i> <i>DG1024</i>	[41]	3

<sup>a</sup> Defined as the percentage of screened clones with the same restriction profile, and, consequently, reasonably corresponding to the same species.

<sup>b</sup> Unpublished data.

7, are equal to  $1.6 \text{ y}^{-1}$  for hydrolysis (resulting in the formation of trichloroethanol) and to  $2.1 \text{ y}^{-1}$  for the elimination reaction (resulting in the formation of TCE) [34,35]. Therefore, the overall abiotic first-order constant accounts for 89% of the first-order depletion constant we evaluated in the sterile microcosms (equal to  $4.1 \text{ y}^{-1}$ ), indicating that losses through caps and other minor abiotic reactions gave a minor contribution to the abiotic 1,1,2,2-TeCA depletion we observed.

### 3.6. Microbiological characterization of a propane-utilizing consortium

Total DNA extracted from the biomass of propane-fed microcosm I-P3 was utilized for the amplification of 16s rDNA with universal primers 27F and 1525R. The amplification products obtained were employed to construct a 16s rDNA gene clone library. Ninety clones were analyzed by restriction fragment length polymorphism (RFLP) as described by Fedi et al. [26]. One clone from each of the ten clone clusters characterized by the same RFLP profile was selected for 16s rDNA sequencing to obtain the phylotype analysis shown in Table 6. Most of the sequenced 16s rDNAs corresponded to the  $\alpha$ -phylogenetic group of the bacterial domain. Several sequences were affiliated to the genus *Roseobacter* and *Sphingomonas*, while others showed high homology with 16S rDNA sequences of uncultured  $\alpha$ -proteobacteria. Most sequences showed similarity with those of bacterial strains isolated from marine environments; of these, some were related to the 16s rDNA sequences of bacteria associated with oceanic algal blooms and playing important roles

in carbon, nitrogen, and sulphur cycling [36]. Some sequences showed a high similarity with those of bacteria involved in the degradation of halogenated solvents [37].

## 4. Conclusions

- The indigenous biomass of the aquifer material investigated in this study proved able to grow on VC 18–43 days (depending on the temperature) after the establishment of aerobic conditions, and to degrade via cometabolism *cis*- and *trans*-DCE but not TCE, 1,1,2-TCA or 1,1,2,2-TeCA present. Conversely, the supply of methane or propane led to the biodegradation of the entire 6-CAH mixture.
- The bioaugmentation treatments, performed with internal inocula obtained from the site's indigenous biomass, were highly effective in reducing the long and variable lag-phases required for the onset of propane or methane uptake in the non-augmented microcosms.
- In all the propane- or methane-fed microcosms the biodegradation of each CAH rapidly reached a stationary condition with higher rates in the low-chlorinated solvents.
- We consider of particular interest the long-term aerobic cometabolic transformation of 1,1,2,2-TeCA by propane-utilizing biomasses.

## Acknowledgments

This research was partly funded with the Protection of Groundwater Resources (PURE) program of the European

Union (Workpackage no. 8, Fifth Framework Program) and with the 2002 and 2003 *Ricerca Fondamentale Orientata* funding of the University of Bologna (Italy). The authors greatly acknowledge Andrea Meniconi, Matteo Balboni, Cecilia Razzetti and Leonardo Fioravanti for their help in the experimental work.

## Appendix A. Supplementary data

Supplementary data associated with this article can be found, in the online version, at doi:10.1016/j.hazmat.2006.05.009.

## References

- [1] H.L. Chang, L. Alvarez-Cohen, Biodegradation of individual and multiple chlorinated aliphatic hydrocarbons by methane-oxidizing cultures, *Appl. Environ. Microbiol.* 62 (1996) 3371–3377.
- [2] Y. Kim, D. Arp, L. Semprini, Kinetic and inhibition studies for the aerobic cometabolism of 1,1,1-trichloroethane, 1,1-dichloroethylene, and 1,1-dichloroethane by a butane-grown mixed culture, *Biotechnol. Bioeng.* 80 (2002) 498–508.
- [3] Y. Kim, D. Arp, L. Semprini, Chlorinated solvent cometabolism by butane-grown mixed culture, *J. Environ. Eng. ASCE* 126 (2000) 934–942.
- [4] L. Meza, T.J. Cutright, B. El-Zahab, P. Wang, Aerobic biodegradation of trichloroethylene using a consortium of five bacterial strains, *Biotechnol. Lett.* 25 (2003) 1925–1932.
- [5] N. Hamamura, C. Page, T. Long, L. Semprini, D.J. Arp, Chloroform cometabolism by butane-grown CF8, *Pseudomonas butanovora* and *Mycobacterium vaccae* job5 and methane-grown *Methylosinus trichosporium* OB3b, *Appl. Environ. Microbiol.* 63 (1997) 3607–3613.
- [6] S. Lonoth, J.D. Semrau, Methane and trichloroethylene degradation by *Methylosinus trichosporium* OB3b expressing particulate methane monooxygenase, *Appl. Environ. Microbiol.* 64 (1998) 1106–1114.
- [7] H.L. Chang, L. Alvarez-Cohen, Transformation capacities of chlorinated organics by mixed cultures enriched on methane, propane, toluene or phenol, *Biotechnol. Bioeng.* 45 (1995) 440–449.
- [8] C.E. Aziz, G. Georgiou, G.E. Speitel Jr., Cometabolism of chlorinated solvents and binary chlorinated solvent mixtures using *M. trichosporium* OB3b PP358, *Biotechnol. Bioeng.* 65 (1999) 100–107.
- [9] L. Alvarez-Cohen, P.L. McCarty, Product toxicity and cometabolic competitive inhibition modeling of chloroform and trichloroethylene transformation by methanotrophic resting cells, *Appl. Environ. Microbiol.* 57 (1991) 1031–1037.
- [10] L.W. Lackey, T.J. Phelps, P.R. Bienkowski, D.C. White, Biodegradation of chlorinated aliphatic hydrocarbon mixtures in a single-pass packed-bed reactor, *Appl. Biochem. Biotechnol.* 39/40 (1993) 701–713.
- [11] J.L. Long, H.D. Stensel, J.H. Ferguson, S.E. Strand, J.E. Ongerth, Anaerobic and aerobic treatment of chlorinated aliphatic compounds, *J. Environ. Eng. ASCE* 119 (1993) 300–320.
- [12] USEPA. Engineered Approaches to In-situ Bioremediation of Chlorinated Solvents: Fundamentals and Field Applications, EPA 542-R-00-008, 2000.
- [13] P.L. McCarty, L. Semprini, Groundwater treatment for chlorinated solvents, in: R.S. Kerr (Ed.), *Environmental Research Laboratory, Handbook of Bioremediation*, Lewis Publishers, Boca Raton, CA, 1994, pp. 87–116.
- [14] C. Chen, J.A. Puhakka, J.F. Ferguson, Transformations of 1,1,2,2-Tetrachloroethane under methanogenic conditions, *Environ. Sci. Technol.* 30 (1996) 542–547.
- [15] M.F. Verce, C.K. Gunsch, A.S. Danko, D.L. Freedman, Cometabolism of *cis*-1,2-dichloroethylene by aerobic cultures grown on vinyl chloride as the primary substrate, *Environ. Sci. Technol.* 36 (2002) 2171–2177.
- [16] N.V. Coleman, T.E. Mattes, J.M. Gossett, J.C. Spain, Biodegradation of *cis*-dichloroethene as the sole carbon source by a  $\beta$ -proteobacterium, *Appl. Environ. Microbiol.* 68 (2002) 2726–2730.
- [17] N.V. Coleman, T.E. Mattes, J.M. Gossett, J.C. Spain, Phylogenetic and kinetic diversity of aerobic vinyl chloride-assimilating bacteria from contaminated sites, *Appl. Environ. Microbiol.* 68 (2002) 6162–6171.
- [18] S. Hartmans, J.A.M. DeBont, Aerobic vinyl chloride metabolism in *Mycobacterium aurum* L1, *Appl. Environ. Microbiol.* 58 (1992) 1220–1226.
- [19] P. Jitnuyanont, L.A. Sayavedra-Soto, L. Semprini, Bioaugmentation of butane-utilizing microorganisms to promote cometabolism of 1,1,1-trichloroethane in groundwater microcosms, *Biodegradation* 12 (2001) 11–22.
- [20] J. Munakata-Marr, V.G. Matheson, L.J. Forney, J.M. Tiedje, P.L. McCarty, Long-term biodegradation of trichloroethylene influenced by bioaugmentation and dissolved oxygen in aquifer microcosms, *Environ. Sci. Technol.* 31 (1997) 786–791.
- [21] R.J. Steffan, K.L. Sperry, M.T. Walsch, S. Vainberg, C.W. Condee, Field-scale evaluation of in-situ bioaugmentation for remediation of chlorinated solvents in groundwater, *Environ. Sci. Technol.* 33 (1999) 2771–2781.
- [22] APHA, Standard Methods for the Examination of Water and Wastewater, 20th ed., American Public Health Association, Washington, DC, 1999.
- [23] R. Sander, Compilation of Henry's Law Constants for Inorganic and Organic Species of Potential Importance in Environmental Chemistry, 1999. <http://www.mpch-mainz.mpg.de/~sander/res/henry.html> (accessed April 2006).
- [24] A. Delle Site, Factors affecting sorption of organic compounds in natural sorbent/water systems and sorption coefficients for selected pollutants. A review, *J. Phys. Chem. Ref. Data* 30 (2001) 187–439.
- [25] D. Frascari, A. Zannoni, S. Fedi, Y. Pii, D. Zannoni, D. Pinelli, M. Nocentini, Aerobic cometabolism of chloroform by butane-grown microorganisms: long-term monitoring of depletion rates and isolation of a high-performing strain, *Biodegradation* 16 (2005) 147–158.
- [26] S. Fedi, V. Tremaroli, D. Scala, J.R. Perez-Jimenez, F. Fava, L. Young, D. Zannoni, T-RFLP analysis of bacterial communities in cyclodextrin-amended bioreactors developed for biodegradation of polychlorinated biphenyls, *Res. Microbiol.* 156 (2005) 201–210.
- [27] Y. Kim, L. Semprini, D. Arp, Aerobic cometabolism of chloroform and 1,1,1-trichloroethane by butane-grown microorganisms, *Bioremediat. J.* 1 (1997) 135–148.
- [28] A. Tovanaboot, L. Semprini, Comparison of TCE transformation abilities of methane- and propane-utilizing microorganisms, *Bioremediat. J.* 2 (1998) 105–124.
- [29] L. Alvarez-Cohen, G.E. Speitel Jr., Kinetics of aerobic cometabolism of chlorinated solvents, *Biodegradation* 12 (2001) 105–126.
- [30] D.J. Arp, C.M. Yeager, M.R. Hyman, Molecular and cellular fundamentals of aerobic cometabolism of trichloroethylene, *Biodegradation* 12 (2001) 81–103.
- [31] R. Oldenhuis, J.Y. Oedzes, J.J. van der Waarde, D.B. Janssen, Kinetics of chlorinated hydrocarbon degradation by *Methylosinus trichosporium* OB3b and toxicity of trichloroethylene, *Appl. Environ. Microbiol.* 57 (1991) 7–14.
- [32] M.M. Lorah, L.D. Olsen, Degradation of 1,1,2,2-tetrachloroethane in a freshwater tidal wetland: field and laboratory evidence, *Environ. Sci. Technol.* 33 (1999) 227–234.
- [33] M.M. Lorah, M.A. Voytek, Degradation of 1,1,2,2-tetrachloroethane and accumulation of vinyl chloride in wetland sediment microcosms and in situ porewater: biogeochemical controls and associations with microbial communities, *J. Contam. Hydrol.* 70 (2004) 117–145.
- [34] P.M. Jeffers, L.M. Ward, L.M. Woytowitch, N.L. Wolfe, Homogeneous hydrolysis rate constants for selected chlorinated methanes, ethanes, ethenes and propanes, *Environ. Sci. Technol.* 23 (1989) 965–969.
- [35] J.A. Joens, R.A. Slifker, E.M. Cadavid, R.D. Martinez, M.G. Nickelsen, W.J. Cooper, Ionic strength and buffer effects in the elimination reaction of 1,1,2,2-tetrachloroethane, *Wat. Res.* 29 (1995) 1924–1928.
- [36] J.M. Gonzalez, R. Simo, R. Massana, J.S. Covert, E.O. Casamayor, C. Pedros-Alio, M.A. Moran, Bacterial community structure associated with a dimethylsulfoniopropionate-producing North Atlantic algal bloom, *Appl. Environ. Microbiol.* 66 (2000) 4237–4246.
- [37] A. Hiraishi, Y. Yonemitsu, M. Matsushita, Y.K. Shin, H. Kuraishi, K. Kawahara, Characterization of *Porphyrobacter sanguineus* sp. nov., an aerobic bacteriochlorophyll-containing bacterium capable of degrading biphenyl and dibenzofuran, *Arch. Microbiol.* 178 (2002) 45–52.

- [38] K. Zengler, G. Toledo, M. Rappe, J. Elkins, E.J. Mathur, J.M. Short, M. Keller, Cultivating the uncultured, Proc. Natl. Acad. Sci. U.S.A. 99 (2002) 15681–15686.
- [39] M. Kolari, J. Nuutinen, F.A. Rainey, M.S. Salkinoja-Salonen, Colored moderately thermophilic bacteria in paper-machine biofilms, J. Ind. Microbiol. Biotechnol. 30 (2003) 225–238.
- [40] G.L. Hold, E.A. Smith, M.S. Rappé, E.W. Maas, E.R.B. Moore, C. Stroempl, J.R. Stephen, J.I. Prosser, T.H. Birkbeck, S. Gallacher, Characterisation of bacterial communities associated with toxic and non-toxic dinoflagellates: *Alexandrium* spp. and *Scrippsiella trochoidea*, FEMS Microb. Ecol. 37 (2001) 161–173.
- [41] D.H. Green, L.E. Llewellyn, A.P. Negri, S.I. Blackburn, C.J.S. Bolch, Phylogenetic and functional diversity of the cultivable bacterial community associated with the paralytic shellfish poisoning dinoflagellate *Gymnodinium catenatum*, FEMS Microb. Ecol. 47 (2004) 345–357.